ACS OMEGA

http://pubs.acs.org/journal/acsodf

Article

Integrating Metabolomics and Network Pharmacology to Explore the Mechanism of Tongmai Yangxin Pills in Ameliorating Doxorubicin-Induced Cardiotoxicity

Lexin Shu,[#] Yuming Wang,[#] Wei Huang,[#] Simiao Fan, Junhua Pan, Qingbo Lv, Lin Wang, Yujing Wang, Jinpeng Xu, Haifeng Yan, Yuchao Bai, Yi Wang,* and Yubo Li*

Cite This: *ACS Omega* 2023, 8, 18128−18139

Read Online

ACCESS | Metrics & More | Article Recommendations | Supporting Information

ABSTRACT: Doxorubicin (DOX) is a broad-spectrum chemotherapeutic drug used in clinical treatment of malignant tumors. It has a high anticancer activity but also high cardiotoxicity. The aim of this study was to explore the mechanism of Tongmai Yangxin pills (TMYXPs) in ameliorating DOX-induced cardiotoxicity through integrated metabolomics and network pharmacology. In this study, first, an ultrahigh-performance liquid chromatography−quadrupole-time-of-flight/mass spectrometry (UPLC−Q-TOF/MS) metabonomics strategy was established to obtain metabolite information and potential biomarkers were determined after data processing. Second, network pharmacological analysis was used to evaluate the active components, drug−disease targets, and key pathways of TMYXPs to alleviate DOX-induced cardiotoxicity. Targets from the network pharmacology analysis and metabolites from plasma metabolomics were jointly analyzed to select crucial metabolic pathways. Finally, the related proteins were verified by integrating the above results and the possible mechanism of TMYXPs to alleviate DOX-induced cardiotoxicity was studied. After metabolomics data processing, 17 different metabolites were screened, and it was found that TMYXPs played a role in myocardial protection mainly by affecting the tricarboxylic acid (TCA) cycle of myocardial cells. A total of 71 targets and 20 related pathways were screened out with network pharmacological analysis. Based on the combined analysis of 71 targets and different metabolites, TMYXPs probably played a role in myocardial protection through regulating upstream proteins of the insulin signaling pathway, MAPK signaling pathway, and p53 signaling pathway, as well as the regulation of metabolites related to energy metabolism. They then further affected the downstream Bax/Bcl-2−Cyt c−caspase-9 axis, inhibiting the myocardial cell apoptosis signaling pathway. The results of this study may contribute to the clinical application of TMYXPs in DOX-induced cardiotoxicity.

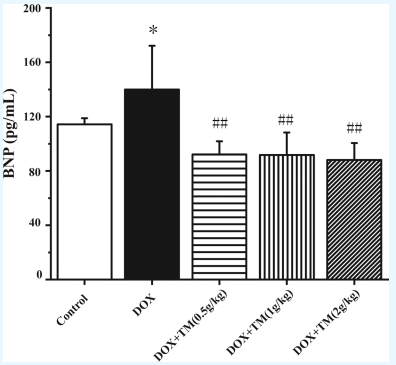

1. INTRODUCTION

Doxorubicin (DOX) is a broad-spectrum chemotherapy drug commonly used in clinical practice to treat a variety of malignant tumors, such as solid tumors, leukemia, lymphoma, and breast cancer.[1] However, DOX can also cause multiple adverse reactions, such as hematopoietic inhibition, malignancy, vomiting, tissue extravasation, and hair loss, thus limiting its wide use to a certain extent. Among them, cardiotoxicity is a common adverse reaction, which is manifested as myocardial cell damage, apoptosis, necrotic cell death, life-threatening left ventricular dysfunction, arrhythmia, and heart failure.[2] Alleviating DOX-induced cardiotoxicity is still a hot current research topic, and it is of great theoretical significance and clinical application value to search for effective cardiotoxicity protective agents.

A Tongmai Yangxin pill (TMYXP) is a traditional Chinese medicine (TCM) formula composed of the following 11 herbs: *Rehmannia glutinosa* (Gaertn.) DC., *Spatholobus suberectus* Dunn, *Ophiopogon japonicus* (Thunb.) Ker Gawl., *Glycyrrhiza uralensis* Fisch., *Polygonum multiflorum* Thunb., *Equus asinus* L., *Schisandra chinensis* (Turcz.) Baill., *Codonopsis pilosula* (Franch.) Nannf., *Chinemys reevesii* (Gray), *Ziziphus jujuba* Mill., and *Cinnamomum cassia* Presl. It was used for treating qi and yin deficiency syndrome resulting from coronary heart disease and arrhythmia.[3] Some studies showed that TMYXP had antioxidant and anti-inflammatory effects,[4] which could regulate the balance of free radicals in cardiomyocytes and reduce apoptosis.[5] Therefore, based on the clinical characteristics of DOX-induced cardiotoxicity and the composition of TMYXP, this study proposed the hypothesis that TMYXP could prevent DOX-induced cardiotoxicity by reducing myocardial cell apoptosis.

Received: March 3, 2023
Accepted: April 25, 2023
Published: May 8, 2023

Metabolomics is a new research field, and its comprehensive view is completely consistent with the overall view of TCM.[6] It can comprehensively describe metabolite changes by the environment and drug effects,[7] and the mechanism of drug action on the body can be explained from the perspective of metabolism.[8] Generation of diseases is often a result of the accumulation of small defects in many genes, so the treatment of a single target cannot be completely effective.[9,10] Through network pharmacology, the target interaction network is used to study the inter-relationship between drugs, organisms, and diseases as a whole, which is common with the idea of the overall regulation and synergistic effect of TCM prescriptions.[11] At present, network pharmacology has been used to predict the targets and pathways and also elucidate the mechanism of action from the protein level of many TCM prescriptions.[12] However, network pharmacology can only be used to predict potential targets and pathways affected by chemical components but not to explain the changes of metabolites in vivo after drug administration, which limited the in-depth study of the mechanism of toxicity.[13] Therefore, this study combined metabolomics and network pharmacology to reveal the mechanism of alleviating DOX-induced cardiotoxicity of TMYXP by reducing apoptosis from the metabolic and molecular levels. First, based on the technology of ultrahigh-performance liquid chromatography−quadrupole-time-of-flight/mass spectrometry (UPLC−Q-TOF/MS), the changes of comprehensive metabolites in vivo DOX model rats after administration of TMYXP were studied to reveal the mechanism of action from metabolites. Then, based on the strategy of multicomponent, multitarget, and multipathway of network pharmacology, potential targets, and signaling pathways were found, and the mechanism of action was explained from the protein level. Finally, the regulation network of chemical constituents−targets−pathways−regulatory indicators−metabolites of the TMYXP alleviating DOX-induced cardiotoxicity was established through integration analysis of metabolomics and network pharmacology, and the mechanism of TMYXP alleviating DOX-induced cardiotoxicity by reducing apoptosis was further elaborated, which provided the reference for the clinical efficacy and safety of TCM.

2. RESULTS

2.1. Serum BNP Content. B-type natriuretic peptide (BNP) is an important index for the diagnosis and treatment of cardiac function. After the experiment, whole blood samples were obtained in heparinized test tubes, and the supernatant was centrifuged twice to obtain plasma samples, some of which were used for the detection of BNP. serum The serum BNP content was increased significantly ($P < 0.05$) for DOX group compared with the control group, while decreased significantly ($P < 0.01$) for the TMYXP group compared to DOX group. (Figure 1).

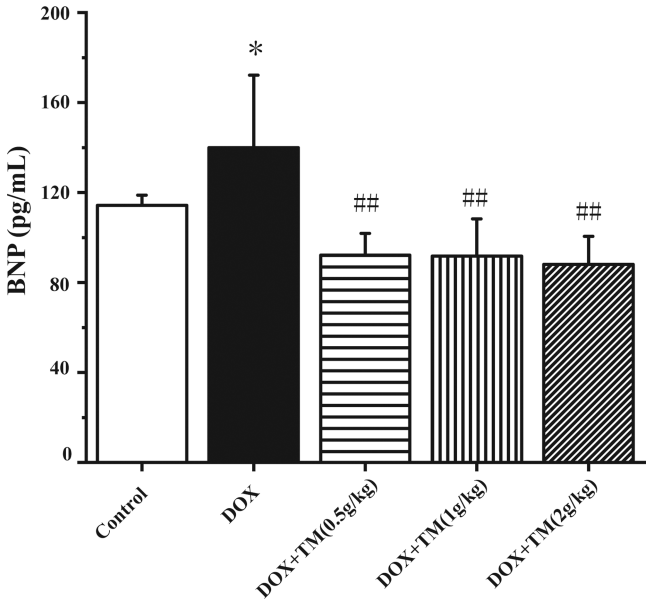

Figure 1. Contents of serum BNP in rats of each group.

2.2. Echocardiographic Analysis. The cardiac function indexes such as ejection fraction (EF), fractional shortening (FS), left ventricular internal diameter end diastole (LVIDd), left ventricular internal diameter end-systole (LVIDs), etc. were measured by an ultrasonic Doppler instrument from the long-axis section of the sternum. Statistical analysis revealed that EF, FS, left ventricular posterior wall thickness systole (LVPWs), and interventricular septum systole (IVSs) in the DOX group were significantly decreased ($P < 0.01$), while LV Vols and LVIDs were significantly increased ($P < 0.01$), compared with those in the control group. In addition, data analysis indicated that EF, FS, and LVPWs of rats in the middle and high-dose groups of TMYXP increased significantly ($P < 0.01$) and LVIDs decreased significantly ($P < 0.01$), compared with those in the model group (Figure 2).

2.3. Histopathological Result of Heart Tissue. Histopathological examination of heart tissue was done to further illustrate DOX-induced cardiotoxicity (Figure 3). The control group exhibited normal morphological findings. However, there were significant changes in the DOX group, including obvious (green arrow) myocardial cell edema, partially visible vacuoles, dissolution and rupture of myocardial fibers, and infiltration of a large number of inflammatory cells in the interstitium. Compared with the DOX group, with the increase of the dose, the degree of myocardial injury was gradually reduced and the edema was significantly reduced. A small infiltration of inflammatory cells and a small amount of interstitial edema with occasional vacuolated cells were also observed. The myocardial cells were relatively complete, and the myocardial tissue was significantly improved, indicating that TMYXP had a protective effect on DOX-induced cardiotoxicity.

2.4. Tunel Fluorescent Staining. Histological section were tested according to TUNEL apoptosis detection kit, and TUNEL staining showed green color for apoptotic cells and blue color for nuclei of normal cells. In this experiment, we could observe that the number of green apoptotic cells was high in the DOX group (Figure 4B), and the number of green apoptotic cells decreased gradually with the increase of the dose of TMYXW administration. Meanwhile, administration of TMYXP reduced apoptotic cells, among which the high-dose group performed the best.

2.5. Metabolomics Analysis in the Plasma Sample. The metabolic spectra of plasma samples in five groups were obtained by UPLC−Q-TOF/MS analysis. The base peak intensity (BPI) diagrams of plasma QC samples in positive and negative ion modes are shown in Supporting Information Figure S1. The results of the methodological investigation showed that the peak area was all less than 15%, and the relative standard deviation (RSD) values of retention time were all less than 3%. The methodological investigation results

https://doi.org/10.1021/acsomega.3c01441
ACS Omega 2023, 8, 18128−18139

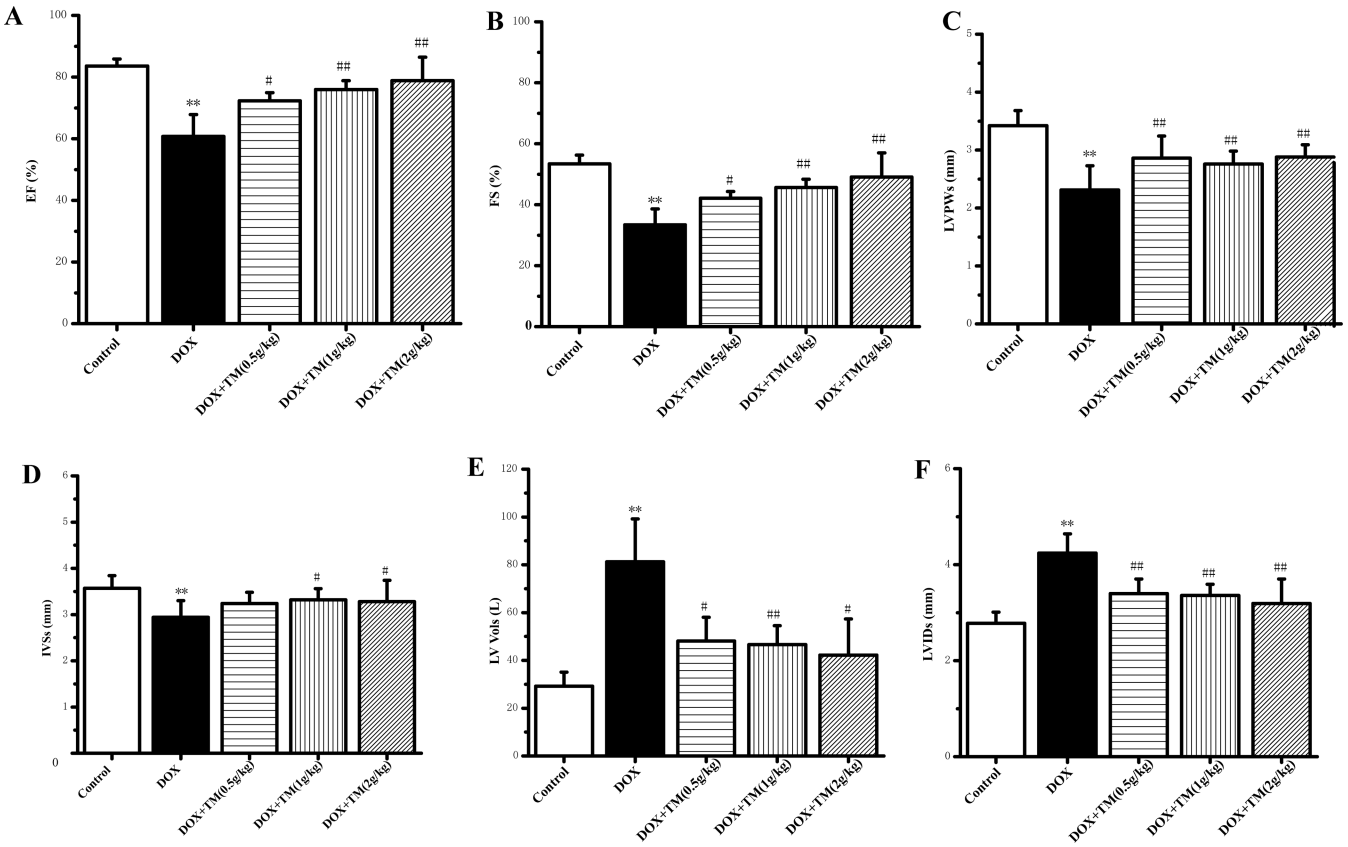

Figure 2. Effect of TMYXP on LV functions following DOX-induced cardiotoxicity. * $P < 0.05$, ** $P < 0.01$, compared with the control group; $^{\#}P < 0.05$, $^{\#\#}P < 0.01$,compared with the DOX group.

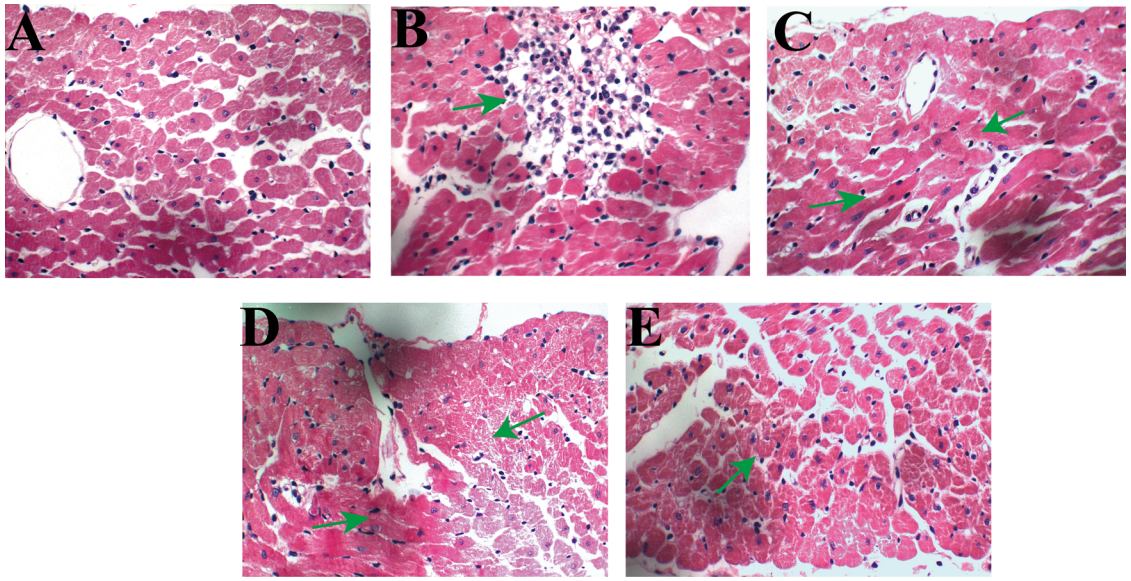

Figure 3. H&E staining was performed on ventricular myocardium to observe histopathologic changes (×400 magnification). (A) Control group, (B) DOX group, (C) DOX + TM (0.5 g/kg) group, (D) DOX + TM (1 g/kg) group, and (E) DOX + TM (2 g/kg) group.

showed that the instrument precision, method precision, and sample stability were reliable.

After preprocessing the data, SIMCA-P software was used to establish the unsupervised principal component analysis (PCA) model for analysis of the five groups of data (Figure 5A1,A2). After removing outliers, the partial least-squares discriminant analysis (PLS-DA) score graph was constructed (Figure 5B1,B2). It can be seen from the figure that the five groups presented good classification aggregation, and there were significant differences between the TMYXP administration group and DOX group and between the TMYXP administration group and the control group, indicating that the endogenous substances in the TMYXP administration group were significantly changed compared with those in the control

https://doi.org/10.1021/acsomega.3c01441
ACS Omega 2023, 8, 18128−18139

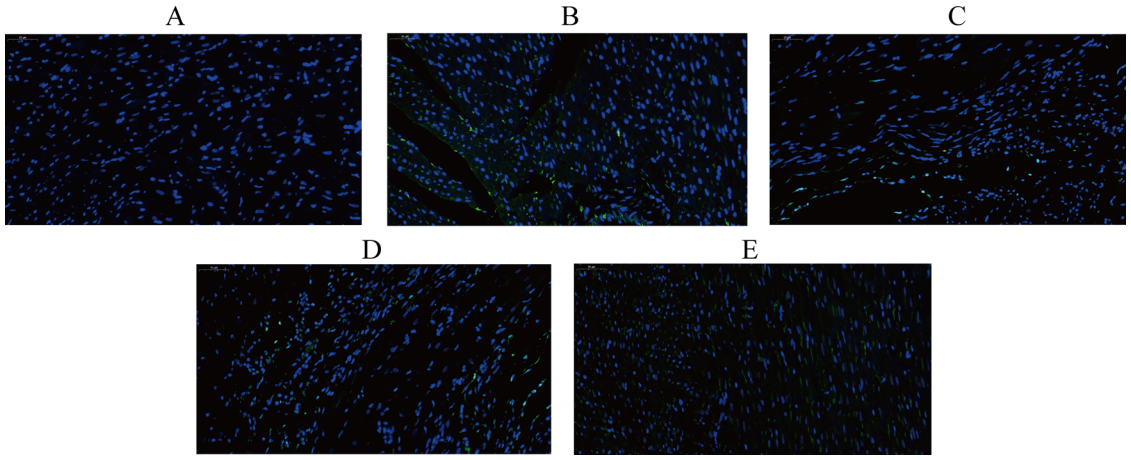

Figure 4. TUNEL staining of TMYXP treatment on DOX-induced myocardial apoptosis (×400 magnification). (A) Control group, (B) DOX group, (C) DOX + TM (0.5 g/kg) group, (D) DOX + TM (1 g/kg) group, and (E) DOX + TM (2 g/kg) group.

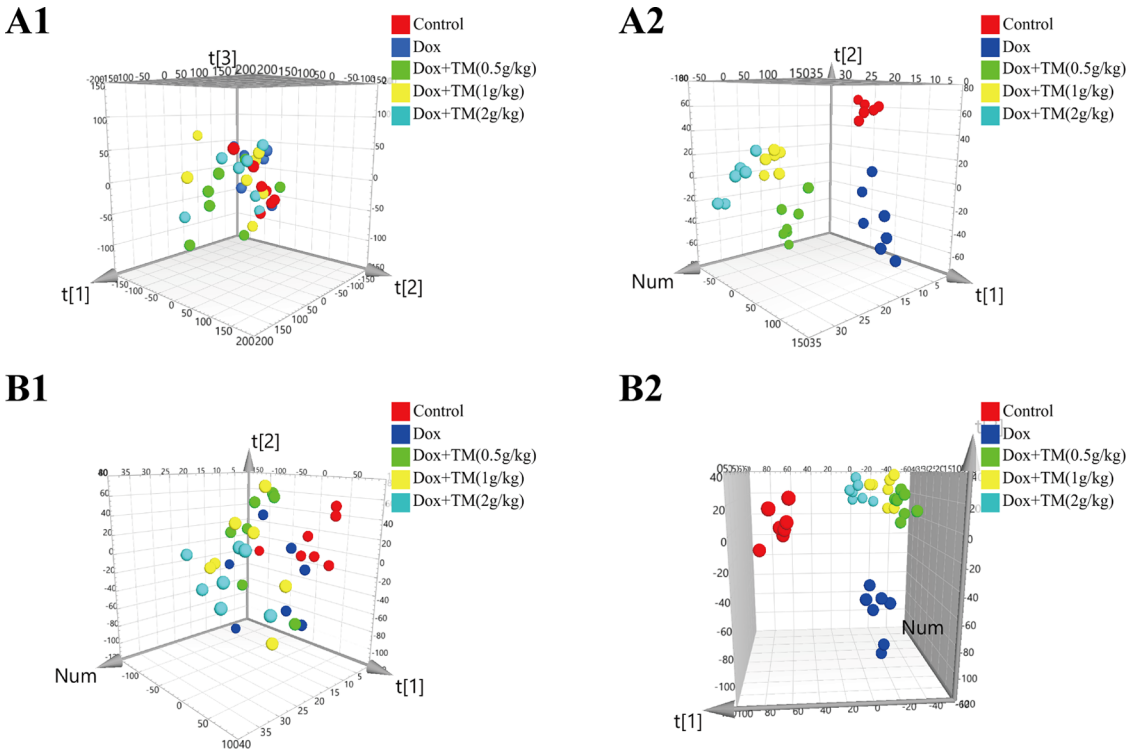

Figure 5. Results of multivariate statistical analysis. (A1) PCA score plot in the positive mode, (A2) PLS-DA score plot in the positive mode, (B1) PCA score plot in the negative mode, and (B2) PLS-DA score plot in the negative mode.

group and DOX group. Then, VIP ≥ 1.5 was selected, and the substance was screened in HMDB and other databases with an adjusted error of 0.01 Da. The substances with significant differences ($P < 0.05$) between the control group and DOX group were screened out by a *t*-test, and the above discriminant metabolites were used as potential biomarkers for the reduction of adriamycin cardiotoxicity by TMYXP.

By searching and comparing the above-mentioned discriminant metabolites in the HMDB database, 17 potential discriminant metabolites of TMYXP for preventing cardiotoxicity of DOX were annotated (Table 1). To explore whether these 17 markers had diagnostic significance, the receiver operating characteristic (ROC) curve was used. The area under each curve (AUC) was used to judge the diagnostic efficiency: the larger the area, the higher the diagnostic value. Through ROC curve analysis, the area under the curve for each marker was greater than 0.7, which indicated a high diagnostic significance (Figure 6A). To show the changing trend of biomarkers more intuitively, the hierarchical cluster analysis method was used to analyze the found biomarkers (Figure 6B). The abscissa was the sample information, and the ordinate was the marker information, and the depth of color in the figure could reflect the content of the biomarker in the sample. It can be seen from the figure that there were significant differences in the content of the 17 biomarkers in the control group and DOX group, indicating that cluster analysis can completely separate the annotated markers and also verify the diagnostic ability of these biomarkers. The 17 biomarkers were then introduced into the MetPA database for metabolic pathway analysis to explore the metabolic mechanism. The metabolic

https://doi.org/10.1021/acsomega.3c01441
ACS Omega 2023, 8, 18128−18139

Table 1. Potential Biomarkers Annotated in the Rat Serum Sample

no.	RT (min)	adduct	compound	molecular formula	calcd m/z	obsd m/z	error (ppm)	M/C	administration group TM-L/M	TM-M/M	TM-H/M
1	2.18	M + H	tryptophan	$C_{11}H_{12}N_2O_2$	205.0977	205.0991	6.83	↓[b]	↑	↑[c]	↑[c]
2	0.83	M + H	pyroglutamine	$C_5H_8N_2O_2$	129.0664	129.0665	0.77	↓[a]	↑	↑	↑
3	7.61	M + H	lysoPC(20:1(11Z))	$C_{28}H_{56}NO_7P$	550.3873	550.3816	10.36	↓[b]	↑[c]	↑	↑
4	5.93	M + H	lysoPC(18:1(11Z))	$C_{26}H_{52}NO_7P$	522.356	522.3583	4.40	↓[a]	↑[c]	↑	↑[c]
5	5.92	M + H	LPC (20:4(8Z,11Z,14Z,17Z))	$C_{28}H_{50}NO_7P$	544.3403	544.3405	0.37	↓[a]	↑	↑	↑
6	5.90	M + H	octadecadienoate	$C_{18}H_{32}O_2$	281.2481	281.2500	6.75	↓[a]	↑	↑	↑
7	0.80	M + Na	glutamine	$C_5H_{10}N_2O_3$	169.0589	169.0599	5.92	↓[b]	↑[d]	↑	↑
8	0.76	M + Na	glucosylceramide	$C_{48}H_{93}NO_8$	834.6799	834.6785	−1.68	↓[a]	↑[d]	↑[d]	↑[d]
9	3.84	M + Na	corticosterone	$C_{21}H_{30}O_4$	369.2042	369.2029	−3.52	↓[a]	↓[c]	↓[c]	↓[c]
10	0.93	M + Na	pantothenic acid	$C_9H_{17}O_5N$	242.1004	242.1013	3.72	↓[a]	↑	↑	↑[d]
11	0.79	M − H	glucose	$C_6H_{12}O_6$	179.0556	179.0568	6.70	↓[a]	↑[c]	↑[c]	↑
12	0.93	M − H	*S*-cysteinosuccinic acid	$C_7H_{11}NO_6S$	236.0229	236.0242	5.51	↓[a]	↑	↑	↑
13	5.27	M − H	docosahexaenoic acid	$C_{22}H_{32}O_2$	327.2324	327.2349	7.64	↑[b]	↓	↓	↓
14	0.92	M − H	prolyl-hydroxyproline	$C_{10}H_{16}N_2O_4$	227.1032	227.1046	6.16	↓[a]	↑	↑	↑
15	2.21	M − H	hydroxyphenylacetylglycine	$C_{10}H_{11}NO_4$	208.0610	208.063	9.61	↓[a]	↑	↑	↑
16	8.64	M − H	12,13-epoxy-9,15-octadecadienoic acid	$C_{18}H_{30}O_3$	293.2117	293.2109	−2.73	↓[a]	↑	↑	↑
17	3.20	M − H	tetradecanedioic acid	$C_{14}H_{26}O_4$	257.1753	257.1778	9.72	↓[a]	↑	↑	↑

[a] $p < 0.05$ compared with the control group. [b] $p < 0.01$ compared with the control group. [c] $p < 0.05$ compared with the model group. [d] $p < 0.01$ compared with the model group. C, control group; M, DOX group; TM-L, TMYXP low-dose group; TM-M, TMYXP middle-dose group; TM-H, TMYXP high-dose group. "↑" or "↓" represents the increased or decreased metabolite.

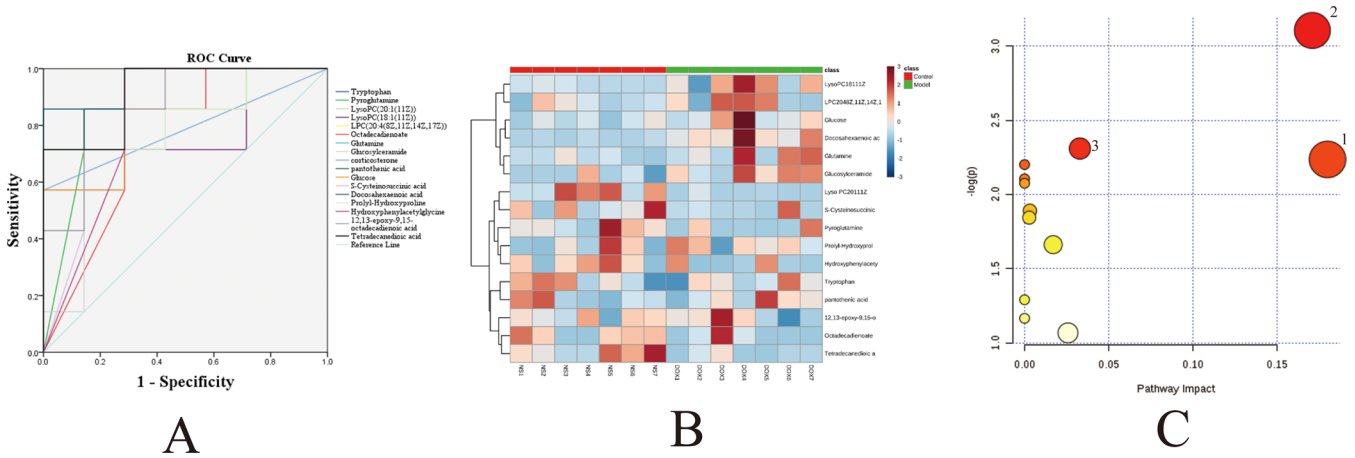

Figure 6. (A) ROC curve of the biomarker; (B) heat map analysis of biomarkers, and (C) disturbed metabolic pathways analyzed by MetPA. Note: (1) pantothenate and CoA biosynthesis, (2) D-glutamine and D-glutamate metabolism, and (3) sphingolipid metabolism.

pathways mainly involved pantothenate and CoA biosynthesis, D-glutamine and D-glutamate metabolism, sphingolipid metabolism, etc. (Figure 6C). 17 biomarkers can affect TCA cycle energy supply through amino acid metabolism, phospholipid metabolism and fatty acid metabolism (Supporting Information: Figure S2). TMYXP can protect myocardium by affecting the TCA cycle.

2.6. Network Pharmacology Analysis. Based on 144 chemical components in TMYXP, a total of 257 target points were predicted through the PharmMapper database, while 119 targets closely related to cardiotoxicity were screened out based on the disease database. Common targets were selected, and repeated targets were removed. Finally, 71 TMYXP−targets were screened out for subsequent pathway enrichment analysis. The predicted targets were corrected using the UniProt (https://www.uniprot.org/) database to exclude nonhuman genes to obtain the potential targets of action of TMYXP chemical components (Supporting information Table S1). Through the analysis of the network of TMYXP−targets, it was found that there were many compounds acting on the same target protein in 144 chemical components, and there were also some monolayers acting on multiple target proteins. For example, mitogen-activated protein kinase 14 can be activated by gancaonin L, isoviolanthin, gomisin D, licorice glycoside A, and other chemical components. Gancaonin L could also act on inositol monophosphatase, cAMP-specific 3,5-cyclicphosphodiesterase 4D, phosphoenolpyruvate carboxykinase, α-1-antitrypsin, and other targets.

Based on the above results, cellular pathways were analyzed by the MAS 3.0 database and the KEGG database, and 13 pathways were identified. Among these, 20 were closely related to cardiotoxicity (Supporting Information Table S2). Pathways related to immune regulation included the B cell receptor signaling pathway, T cell receptor signaling pathway, Toll-like receptor signaling pathway, and JAK−STAT signaling pathway. Pathways related to coagulation were complement and coagulation cascades. Inflammatory pathways included the vascular endothelial growth factor signaling pathway and

https://doi.org/10.1021/acsomega.3c01441
ACS Omega 2023, 8, 18128−18139

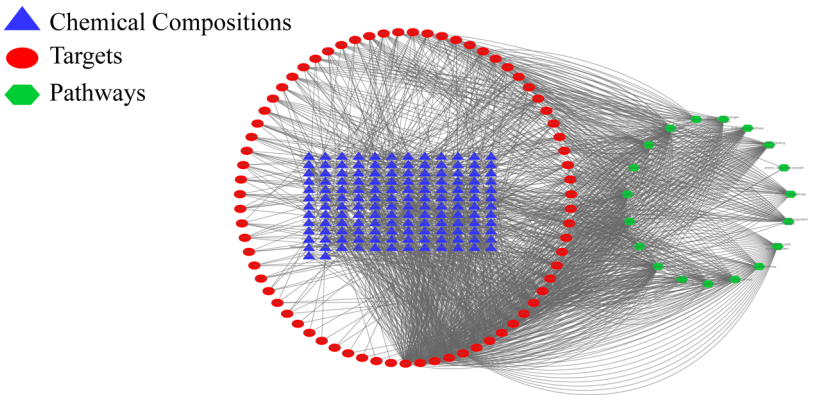

Figure 7. Composition−target−pathway regulatory network of TMYXP.

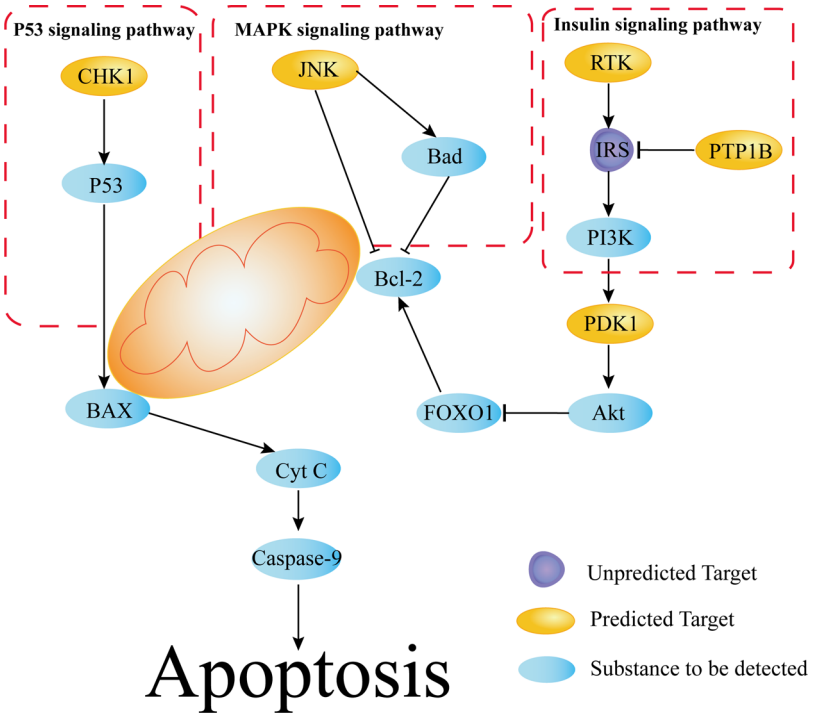

Figure 8. Network pharmacologic pathway analysis of TMYXP.

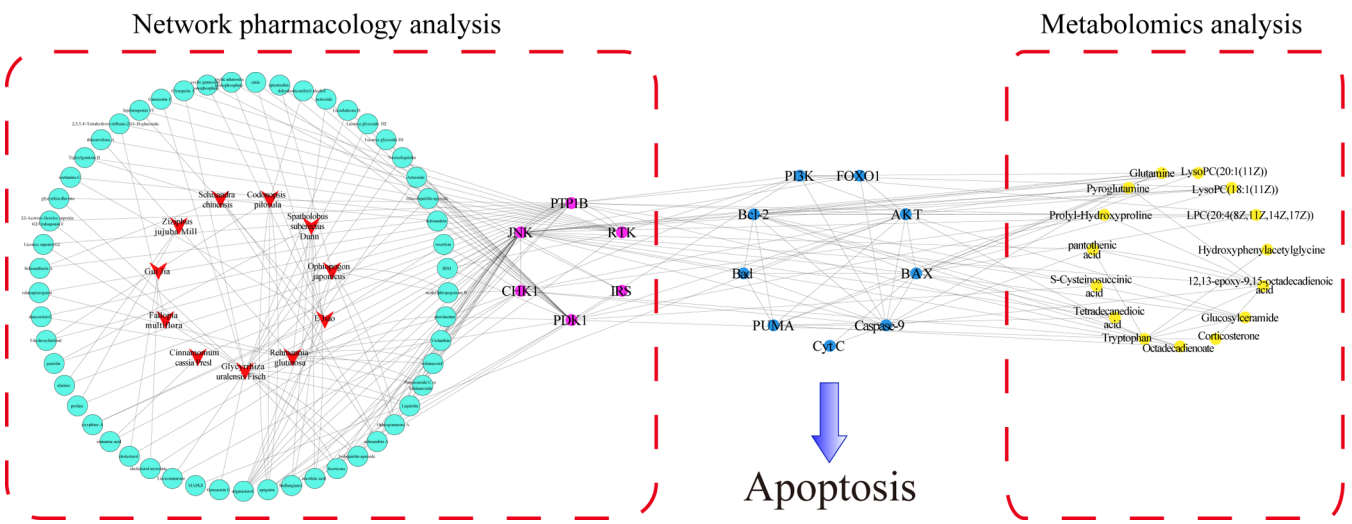

Figure 9. Network pharmacology prediction and metabolomics analysis.

https://doi.org/10.1021/acsomega.3c01441
ACS Omega 2023, 8, 18128−18139

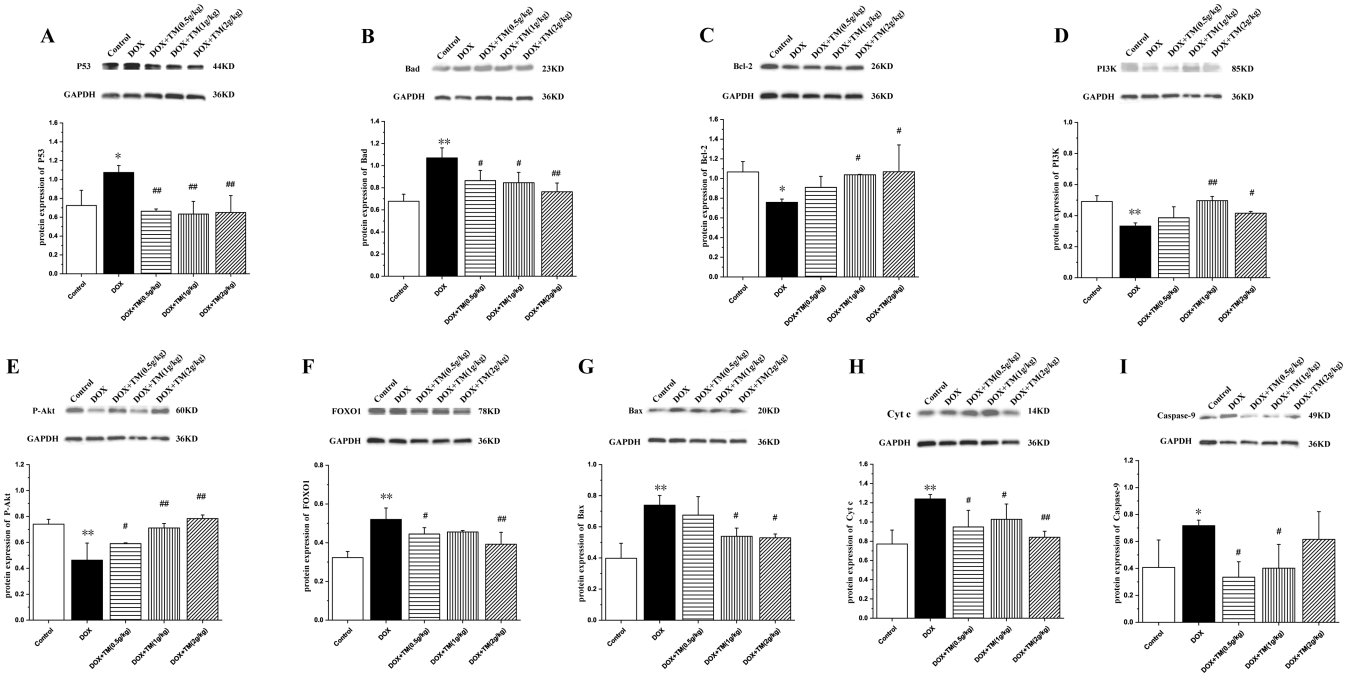

Figure 10. Western blotting band and grayscale analysis of p53 (A), Bad (B), Bcl-2 (C), PI3K (D), P-Akt (E), FOXO1 (F), Bax(G), Cyt c (H), and caspase-9 (I).

MAPK signaling pathway. Pathways related to cell metabolism and apoptosis included the insulin signaling pathway and the p53 signaling pathway. Finally, Cytoscape software was used to establish the network diagram of the chemical constituent−target−pathway (Figure 7), which visually presented the network of constituent−target−pathway of TMYXP to ameliorate DOX-induced cardiotoxicity.

According to the above results, 65 components of TMYXP predicted the insulin signaling pathway, 25 components predicted the p53 signaling pathway, and 37 components jointly predicted the MAPK signaling pathway. KEGG database annotation of this article 3 signaling pathways found that the three downstream pathways were closely related to cell apoptosis. Therefore, a preliminary mechanism may be predicted that TMYXP ameliorated DOX-induced cardiotoxicity by regulating the upstream proteins of the insulin signaling pathway, MAPK signaling pathway, and p53 signaling pathway and then regulating the expression of the downstream apoptosis-related factors, which can reduce the apoptosis of cardiomyocytes and play a role in myocardial protection (Figure 8).

2.7. Network Pharmacology and Metabolomics Integration Analysis. The main target proteins in the MAPK signaling pathway, insulin signaling pathway, and p53 signaling pathway were screened out with the network pharmacology analysis, and the downstream of these target proteins was found to be the apoptosis signaling pathway in the KEGG database signaling pathway diagram. According to the result of the above metabolomics analysis, the 17 metabolites were closely related to the TCA cycle. When *apoptosis* was used as a keyword to be cross searched with the TCA cycle, amino acid metabolism, phospholipid metabolism, and fatty acid metabolism as keywords, 248, 143, 62, and 237 references were obtained, respectively. The results showed that the change of the metabolites can directly or indirectly influence the apoptosis pathway of Bcl-2, Bax, and Cyt c protein expression, and the corresponding relationship was constructed in Cytoscape software (Figure 9). The results showed that metabolomics and network pharmacology were closely related to the proteins of the apoptosis pathway; that is, TMYXP reduced DOX-induced cardiotoxicity by affecting the apoptosis-related proteins and inhibiting the apoptosis.

2.8. Western Blotting Analysis. To verify the above results, the related effector proteins were verified in this study. Western blotting was used to detect the expression of p53, Bcl-2, Bad, PI3K, P-Akt, FOXO1, Bax, Cyt c, and caspase-9 in the heart tissues of rats in each group. As shown in Figure 10, the expression levels of p53, Bad, FOXO1, Bax, Cyt c, and caspase-9 were significantly increased ($P < 0.05$) in the DOX group compared with those in the control group, while these protein expression changes were attenuated by treatment with TMYXP. Compared with those in the control group, the expression levels of PI3K, P-Akt, and Bcl-2 were significantly decreased ($P < 0.05$) in the DOX group, while these protein expression changes were differentially regulated by treatment with TMYXP. The above results showed that the possible mechanism of TMYXP reducing DOX-induced cardiotoxicity was mainly by regulating the upstream proteins of the insulin signaling pathway, MAPK signaling pathway, and p53 signaling pathway and then regulating the expression of downstream apoptosis-related proteins Bcl-2, Bax, Cyt c, and caspase-9, which inhibited the damage to the mitochondrial outer membrane in cardiomyocytes and reduced the apoptosis of cardiomyocytes and thus played a role in myocardial protection.

3. DISCUSSION

Metabolomics studies showed that the 17 discriminant metabolites were mainly amino acids, phospholipids, and fatty acids. In the amino acid group, compared with the control group, the discriminant metabolites such as tryptophan, glutamine amide, and pantothenic acid exhibited different

https://doi.org/10.1021/acsomega.3c01441
ACS Omega 2023, 8, 18128−18139

degrees of downregulation in the DOX group, and these metabolites had different degrees of callback in the TMYXP group. As an energy-intensive organ, the heart normally supplies energy to maintain ion transport, calcium homeostasis, and sarcolemma functions mainly by fatty acids and carbohydrates, and at the same time, it also uses amino acids, lactic acid, and other energy supplies.[14] The TCA cycle is one of the main pathways of energy metabolism in the body, and interference with the TCA cycle may imply decreased oxidative metabolism and impaired the mitochondrial respiratory chain in cardiomyocytes.[15,16] Therefore, when the TCA cycle is inhibited, ATP synthesis of cardiomyocytes is reduced, resulting in energy shortage and cell apoptosis, namely, the generation of cardiotoxicity. Among them, because the intermediate products of the TCA cycle only consist of amino acids, amino acids play a crucial role in myocardial energy metabolism.[17] Tryptophan, as an essential amino acid *in vivo*, plays an important role through metabolic pathways and metabolites.[18] Studies have shown that the reduced plasma tryptophan content in individuals with coronary heart disease is associated with inflammation.[19] When the body is stable and healthy, glutamine is the most abundant amino acid, while when the content of glutamine decreases, the body's antioxidant capacity will be reduced, and the body is vulnerable to infection and immune response.[20] In addition, glutamine can significantly reduce JNK phosphorylation and caspase-9 activity to reduce apoptosis.[21] It can also reduce JNK protein activity by increasing glutathione synthesis, preventing mitochondrial translocation, and inhibiting apoptosis.[22] The metabolite pantothenic acid enters the TCA cycle through conversion to CoA for energy metabolism. If the conversion process of pantothenic acid to CoA is inhibited, the synthesis of glutathione is inhibited, the phosphorylation of JNK protein is increased, and then apoptosis will be induced.[23] In this study, amino acids in the DOX group showed a downward trend, while those in the TMYXP group showed an upregulated trend, indicating that TMYXP could protect amino acid metabolism of cardiomyocytes.

Phospholipids, compared with the control group, were downregulated to a different extent in the DOX group and had a callback in the TMYXP group. Under normal physiological conditions, most of the energy of myocardium comes from fatty acid metabolism. Through literature research, it was found that free fatty acids could affect JNK and PUMA proteins and then affect downstream proapoptotic proteins Bcl-2, Bim, and Bax, which caused mitochondrial apoptotic pathways, leading to the occurrence of fat apoptosis.[24,25] In addition, free fatty acids can also be metabolized into phospholipids, which can be derived into LPC metabolites. Part of LPC is a component of oxidized low-density lipoproteins. It is widely distributed and has a variety of biological effects. It participates in a variety of physiological activities and is involved in the pathogenesis of atherosclerosis and inflammation. The onset of apoptosis is induced by activation of the p38−MAPK pathway,[26] which activates extracellular signal-regulated kinase 1/2 (ERK1/2) and C-Jun N, N-terminal kinase (JNK). Another study has shown that PI3K/Akt signaling plays a critical role in LPC-induced vascular endothelial cell apoptosis and inflammatory response, which can be achieved through Bax, caspase-3, Bcl-2, and Akt proteins.[27,28] It is suggested that after the action of TMYXP on the organism, it affected fatty acid-β oxidation and glycerophospholipid metabolism by increasing myocardial energy supply and thus affected the downstream apoptosis-related proteins to play a protective role in the heart.

Compared with the control group, the discriminant metabolite glucosylceramide was downregulated in the DOX group, and these metabolites had a significant callback in the TMYXP group. Sphingolipids are a class of bioactive lipids that mediate many key cellular processes, including apoptosis and autophagy, and their metabolites have different regulatory effects on the induction of apoptosis and autophagy.[29] Glucosylceramide is used to synthesize sphingolipids by a glycosylation reaction on Golgi bodies. Sphingolipids have been shown to be associated with cell growth, cell signaling, cell differentiation, autophagy, cell death, cell migration, immune response, and inflammatory response. At the same time, the synthesis and metabolism of glucosylceramide need to be completed by ceramide.[30] Ceramide can also be involved in inducing and inhibiting cell apoptosis. In the plasma membrane, ceramide formed by palmitate metabolism can activate PP2A phosphatase, leading to the dephosphorylation and inactivation of Akt and antiapoptotic Bcl-2 protein. In addition, mitochondrial ceramide can also promote the activity of proapoptotic protein Bax.[31] Glucosylceramide decreased in the DOX group, disrupting the balance of glycosyllipid synthesis and metabolism on the golgiosome. Glucosylceramide produced a large amount of ceramide, which led to the dephosphorylation and inactivation of Akt and the inactivation of antiapoptotic Bcl-2 protein or the apoptosis of myocardial cells by promoting the activity of the proapoptotic Bax protein. Glucosylceramide was significantly increased in the TMYXP group, indicating that TMYXP acted on the body to inhibit cell apoptosis, thus playing a protective role in the heart.

Network pharmacology provides a unique and innovative way to study the mechanism of multiple ingredients.[32] In this study, the proteins enriched in the MAPK signaling pathway, insulin signaling pathway, and p53 signaling pathway were closely related to apoptosis, and the effector proteins had been verified. Apoptotic pathways can be roughly divided into the mitochondrial pathway and death receptor pathway, among which the mitochondrial pathway is a response to cell stress and can lead to the activation of proapoptotic protein Bim, which can directly or indirectly activate apoptotic factor Bax and lead to apoptosis.[33,34] In this study, RTK, IRS, and PDK1 proteins in the insulin signaling pathway were predicted, while Bim proteins were downstream of the insulin signaling pathway. Effector proteins PI3K, Akt, and FOXO1 were verified in the western blotting experiment, and the callback trend in the results could prove that TMYXP reduced the apoptosis of cardiomyocytes through the PI3K/FOXO1/Bim/Bax axis. In addition, it was mentioned in the literature that anisomycin could activate Bax and induce apoptosis by phosphorylation of JNK and Bim, of which the JNK protein was predicted in this study and could induce apoptosis by the downstream Bcl-2 protein.[35] p53 is one of the important tumor suppressor genes, and activation of p53 and its downstream targets to induce apoptosis is considered tumor therapy.[36] Shikonin can resist TRAIL bile duct cancer cell apoptosis through p53/PUMA/Bax signal transduction.[37] In this study, network pharmacology predicted the JNK protein downstream of the MAPK signaling pathway and the CHK1 protein upstream of the p53 signaling pathway, and the two signaling pathways had a common downstream protein Bcl-2. Analysis of WB results revealed that the Bcl-2 callback occurred after the administration of TMYXP; that is, TMYXP could reduce

https://doi.org/10.1021/acsomega.3c01441
ACS Omega 2023, 8, 18128−18139

myocardial cell apoptosis through JNK/Bcl-2 /Bax signal transduction and p53/Bcl-2/Bax transduction. Moreover, Bim, Bcl-2, and Bax were all apoptotic factors on the mitochondrial outer membrane.[38,39] Therefore, it is concluded that TMYXP plays a myocardial protective role by inhibiting the damage to the mitochondrial outer membrane in cardiomyocytes and reducing the apoptosis of cardiomyocytes.

4. CONCLUSIONS

In this study, first, 17 discriminant metabolic markers were screened by metabolomics, and it was found that TMYXP could protect the myocardium by affecting the TCA cycle energy supply of cardiomyocytes through amino acid metabolism, phospholipid metabolism, and fatty acid metabolism, and these metabolites were also closely related to apoptosis-related factors. Second, through network pharmacology, it was found that TMYXP could affect the downstream apoptosis-related factors by regulating the main target proteins of the insulin signaling pathway, MAPK signaling pathway, and p53 signaling pathway. Finally, by integrating the above results, it was found that the mechanism of TMYXP to reduce DOX-induced cardiotoxicity was by regulating the upstream proteins of the insulin signaling pathway, MAPK signaling pathway, and p53 signaling pathway and regulating metabolites related to energy metabolism. TMYXP affected the downstream Bax/Bcl-2−Cyt c−caspase-9 axis, inhibited mitochondrial outer membrane damage in myocardial cells, protected the TCA cycle of myocardial cells, and reduced myocardial cell apoptosis to achieve myocardial protection. In this study, network pharmacology and metabolomics were combined to study the mechanism of TMYXP to reduce DOX-induced cardiotoxicity at the molecular and metabolic levels. It may be concluded that TMYXP provided an effective approach and strategy for the treatment of DOX-induced cardiotoxicity in the clinic.

5. MATERIALS AND METHODS

5.1. Chemicals and Reagents. A Waters Acquity UPLC liquid chromatograph (Waters), a Waters Xevo G2 Q-TOF mass spectrometer (Waters), an ACQUITY UPLC BEH C_{18} column (2.1 mm × 100 mm × 1.7 μm) (Waters) were used. Antibodies against GAPDH, P-Akt (Thr308), PI3K, Bax, and Bcl-2 were obtained from Cell Signaling Technology (Beverly, MA). Cyt c, p53, and FOXO1 were purchased from USCN Business Co., Ltd. (Wuhan, China), and Bad was purchased from Proteintech Group Inc. (Wuhan, China). All secondary antibodies (HRP-conjugated antirabbit and antimouse IgG) were obtained from Cell Signaling Technology. The rat serum BNP ELISA kit was purchased from Equation Biotechnology Co., Ltd. (Beijing, China). The BCA Protein Quantification kit was purchased from Cell Signaling Technology. DOX and sodium carboxymethyl cellulose were purchased from Solarbio Co., Ltd. (Beijing, China). Methanol, acetonitrile, and formic acid of HPLC grade were purchased from Merck (Darmstadt, Germany). Pure water was purchased from Watsons (China).

5.2. Drug Preparation. TMYXP (Batch no. 1070353) was provided by Tianjin Zhongxin Pharmaceutical Group Co., Ltd., Lerentang Pharmaceutical Factory (Tianjin, China). The prescription and preparation of TMYXP are consistent with the Chinese Pharmacopoeia (2020 Edition). According to the Chinese Pharmacopoeia (2020 edition), glycyrrhizic acid was quantified for quality control.

UPLC−Q-TOF-MS/MS techniques were used to analyze the chemical constituents of TMYXP (Figure S1). Eighty compounds of TMYXP including flavonoids, coumarins, iridoid glycosides, saponins, and lignans were annotated unambiguously or tentatively.[40]

5.3. Animals and Experimental Design. The animal experiments were approved by the Animal Ethics Committee of Tianjin University of Traditional Chinese Medicine. Male Wistar rats (180−200 g) were purchased from Beijing Weitong Lihua Technology Co., Ltd. (quality certification number: SCXK (Jing)2016-0006). The growth environment consisted of 12 h day/night cycles; ambient temperature was 23 ± 2 °C, with 35 ± 5% humidity. All experiments were carried out in accordance with Chinese national laws and local guidelines. Rats were acclimated for 7 days before the study. A total of 78 rats were randomly divided into five groups: control group (0.5% CMC-Na, 10 mL/kg), DOX group (0.5% CMC-Na, 10 mL/kg), DOX + TM group (0.5 g/kg), DOX + TM group (1 g/kg), and DOX + TM group (2 g/kg). The control group received saline intraperitoneally, and the other groups were given an injection of DOX (3 mg/kg) once a week for 6 weeks to achieve an accumulative dose of 18 mg/kg. At the same time, TMYXP was freshly prepared in 0.5% CMC-Na and orally administered once daily over a period of 6 weeks.

After 1 week of observation, rats were initially anesthetized with 2−3% isoflurane (Fischer Scientific) and then echocardiography was performed. Left ventricular function was assessed using a Vevo2100 small animal ultrasound real-time imaging system (Visual Sonics, Canada).

5.4. Metabolomics Analysis. *5.4.1. Preparation of Plasma Samples.* The plasma samples frozen in a refrigerator at −80 °C were taken out and thawed at room temperature. One hundred microliters of plasma samples were mixed with 300 μL of acetonitrile for protein precipitation. After 10 min of ultrasound in an ice−water bath, the mixture was swirled and mixed for 1 min. The mixture was centrifuged at 13,000 rpm for 15 min at 4 °C, and the supernatants were analyzed by UPLC−Q-TOF/MS. Then, QC samples were prepared according to the above operations for methodological investigation of metabonomics. The above samples were taken for detection in the positive and negative ion modes, respectively.

Rat heart tissues were obtained after normal saline perfusion. Several rat heart tissues were randomly selected and fixed with 10% formaldehyde for hematoxylin−eosin (H&E) staining and TUNEL fluorescence staining, while the rest of the heart tissues were frozen at −80 °C for subsequent western blotting analysis.

5.4.2. UPLC−Q-TOF/MS Analysis. Chromatographic conditions: ACQUITY UPLC BEH C_{18} columns (2.1 mm × 100 mm, 1.7 μm, Waters); injection volume, 5 μL; column temperature, 45 °C; flow rate, 0.3 mL/min; mobile phase composition, phase A was 0.1% formic acid/water, phase B was 0.1% formic acid/acetonitrile; elution conditions: 0−0.5 min, 1%B; 0.5−2 min, 1−50%B; 2−9 min, 50−99%B; 9−10 min, 99%B; 10−11 min, 99−1%B; 11−13 min, 1%B.

Mass spectrometry analysis conditions: ESI was used for mass spectrometry analysis in positive and negative ion ionization modes. Reference ions ($[M + H]^+$ = 556.2771, $[M - H]^-$ = 554.2615) were used to ensure the accuracy of data collection. The scanning range was set at 50−1000 Da; the capillary voltage was 3.0 kV; the ionization source temperature was 100 °C; the desolvation temperature was

https://doi.org/10.1021/acsomega.3c01441
ACS Omega 2023, 8, 18128−18139

400 °C; the desolvation gas flow was 800 L/h; the cone gas flow was 50 L/h; and the gas flow was 0.3 mL/min.

5.4.3. Statistical Analysis. In this study, the serum samples of rats were analyzed by UPLC−Q-TOF/MS. The obtained data were exported by MarkerLynx (version 4.1), and the obtained strength of each ion was normalized to the total number of ions. The derived data included retention time, m/z value, and normalized peak area. The RSD values of peak area and retention time were calculated by randomly selecting 20 peaks from the obtained QC sample profiles. After 80% modification of the data, the multivariate data analysis was performed using SIMICA-P 13.0 software (Umetrics, Sweden) to establish PCA and PLS-DA models. On the basis of the PLS-DA model, compounds with significant contributions to the classification were screened out (VIP > 1.5), and the substances with $P < 0.05$ were further screened out by a t-test. Subsequently, the selected markers were searched and screened in the HMDB (http://www.hmdb.ca/) database according to the first-level debris information to determine the biomarkers of TMYXP to prevent DOX-induced cardiotoxicity.

In addition, the trends of the markers were analyzed by heat map and subject operating characteristic curve (ROC). Finally, the identified biomarkers were analyzed for metabolic pathways through the MetaboAnalyst (https://www.metaboanalyst.ca/) database.

5.5. Network Pharmacology Study of TMYXP. Through literature research, 144 chemical components in TMYXP (Supporting Information: Table S3) were obtained for subsequent network pharmacology research. First, three-dimensional (3D) structures were drawn and stored in the .sdf format. The PharmMapper server was used for potential target prediction analysis. Target proteins with the first ten fit values were selected from the results for subsequent analysis. At the same time, targets related to cardiotoxicity were obtained from the CTD (http://ctdbase.org/), TTD (http://bidd.nus.edu.sg/group/cjttd/), Genecard (https://www.genecards.org/), and OMIM (http://www.omim.org/databases. After matching with the above constituents-targets, the same target was removed, and finally TMYXP − targets were obtained. Then, the above TMYXP − targets were imported into MAS 3.0 database) databases. After matching with the above constituents−targets, the same target was removed, and finally, TMYXP−targets were obtained. Then, the above TMYXP−targets were imported into the MAS 3.0 database to get related pathways for targets, and the selection of the top channel was analyzed. Finally, the chemical components of TMYXP, TMYXP−targets, and the potential signaling pathway were imported into Cytoscape version 3.4.1 to jointly construct the chemical constituent−target−pathway network of TMYXP for ameliorating DOX-induced cardiotoxicity. Then, the screening biomarkers from metabonomics were imported into the Pubmed database (https://www.ncbi.nlm.nih.gov/pubmed/) for literature investigation, getting the metabolite−target network of TMYXP for ameliorating DOX-induced cardiotoxicity, integration of the above results in Cytoscape version 3.4.1, screening the same proteins and pathways for subsequent validation.

5.6. Western Blotting Analysis. Protein extraction and western blotting were performed using standard procedures. Heart tissue was homogenized and quantified with BCA kits. Equal amount of samples were separated by 10% SDS-PAGE gel, transferred to PVDF membranes, and then blocked with 5% nonfat milk. Subsequently, the membranes were incubated with appropriate primary antibodies overnight at 4 °C, followed by TBST washing and incubation with secondary antibodies for 2 h. After cleaning, 200 μL of luminous fluid for the UVP chemiluminescence reaction was added and photographed by an Amersham Imager 600 (GE).

5.7. Statistical Analyses. Data were presented as mean ± SD and analyzed by SPSS software. The statistical significances among groups were analyzed by one-way ANOVA, followed by the Newman−Keuls test. $P < 0.05$ was considered statistically significant.

■ ASSOCIATED CONTENT

Supporting Information

The Supporting Information is available free of charge at https://pubs.acs.org/doi/10.1021/acsomega.3c01441.

BPI diagram of plasma QC samples in positive and negative ion modes (Figure S1), metabolic pathway information (Figure S2), TMYXP major active ingredient related target (Table S1), main pathways of Tongmai Yangxin pills (Table S2), and chemical composition of Tongmai Yangxin pills (Table S3) (PDF)

■ AUTHOR INFORMATION

Corresponding Authors

Yi Wang − *Institute of Traditional Chinese Medicine, Tianjin University of Traditional Chinese Medicine, Tianjin 301617, China*; Phone: +86-22-59596572; Email: wangyi@tjutcm.edu.cn

Yubo Li − *School of Chinese Materia Medica, Tianjin University of Traditional Chinese Medicine, Tianjin 301617, China*; orcid.org/0000-0003-0455-0969; Phone: +86-22-59591974; Email: yaowufenxi@sina.com

Authors

Lexin Shu − *School of Chinese Materia Medica, Tianjin University of Traditional Chinese Medicine, Tianjin 301617, China*

Yuming Wang − *School of Chinese Materia Medica, Tianjin University of Traditional Chinese Medicine, Tianjin 301617, China*

Wei Huang − *School of Chinese Materia Medica, Tianjin University of Traditional Chinese Medicine, Tianjin 301617, China*

Simiao Fan − *School of Chinese Materia Medica, Tianjin University of Traditional Chinese Medicine, Tianjin 301617, China*

Junhua Pan − *Hainan Province Key Laboratory for Drug Preclinical Study of Pharmacology and Toxicology Research, Hainan Medical University, Haikou 571199, China*

Qingbo Lv − *Institute of Traditional Chinese Medicine, Tianjin University of Traditional Chinese Medicine, Tianjin 301617, China*

Lin Wang − *Tianjin Zhongxin Pharmaceutical Group Co., Ltd., Le Ren Tang Pharmaceutical Factory, Tianjin 301617, China*

Yujing Wang − *Tianjin Zhongxin Pharmaceutical Group Co., Ltd., Le Ren Tang Pharmaceutical Factory, Tianjin 301617, China*

Jinpeng Xu − *Tianjin Zhongxin Pharmaceutical Group Co., Ltd., Tianjin 301617, China*

https://doi.org/10.1021/acsomega.3c01441
ACS Omega 2023, 8, 18128−18139

Haifeng Yan − *Institute of Traditional Chinese Medicine, Tianjin University of Traditional Chinese Medicine, Tianjin 301617, China*

Yuchao Bai − *School of Chinese Materia Medica, Tianjin University of Traditional Chinese Medicine, Tianjin 301617, China*

Complete contact information is available at: https://pubs.acs.org/10.1021/acsomega.3c01441

Author Contributions

#L.S., Y.W., and W.H. contributed equally to this work.

Notes

The authors declare no competing financial interest.

■ ACKNOWLEDGMENTS

This work has been supported by the National Natural Science Foundation of China (Nos. 82204799, 81903938, and 81873194) and the Tianjin Development Program for Innovation and Entrepreneurship.

■ ABBREVIATIONS

BNP, brain natriuretic peptide; Cyt c, cytochrome C; DOX, doxorubicin; ESI, electrospray ionization; EF, ejection fraction; FS, fractional shortening; FOXO1, Forkhead box protein O1; GAPDH, glyceraldehydes-3-phosphate dehydrogenase; H&E, hematoxylin−eosin; HMDB, human metabolome database; IVSs, interventricular septum thickness at end-systole; JNK, c-Jun N-terminal kinase; KEGG, Kyoto Encyclopedia of Genes and Genomes; LV Vol, left ventricular end-systolic volume; LVIDs, left ventricular internal diameter at end-systole; LVPWs, left ventricular posterior wall at end-systole; MAPK, mitogen-activated proteinkinase; PCA, principal component analysis; PLS-DA, partial least-squares discriminant analysis; PVDF, poly(vinylidenefluoride); QC, quality control; SDS-PAGE, sodium dodecyl sulfate-polyacrylamide gel electrophoresis; TCA, tricarboxylic acid; TCM, traditional Chinese medicine; TMYXPs, Tongmai Yangxin pills; UPLC−Q/TOF-MS, ultrahigh-pressure liquid chromatography−quadrupole time-of-flight mass spectrometry

■ REFERENCES

(1) Bagchi, D.; Bagchi, M.; Hassoun, E. A.; Kelly, J.; Stohs, S. J. Adriamycin-induced hepatic and myocardial lipid peroxidation and DNA damage, and enhanced excretion of urinary lipid metabolites in rats. *Toxicology* **1995**, *95*, 1−9.

(2) Li, W.; Wang, X.; Liu, T.; Zhang, Q.; Cao, J.; Jiang, Y.; Sun, Q.; Li, C.; Wang, W.; Wang, Y. Harpagoside Protects Against Doxorubicin-Induced Cardiotoxicity via P53-Parkin-Mediated Mitophagy. *Front. Cell Dev. Biol.* **2022**, *10*, No. 813370.

(3) Fan, Y.; Man, S.; Li, H.; Liu, Y.; Liu, Z.; Gao, W. Analysis of bioactive components and pharmacokinetic study of herb-herb interactions in the traditional Chinese patent medicine Tongmai Yangxin Pill. *J. Pharm. Biomed. Anal.* **2016**, *120*, 364−373.

(4) Wang, Y.; Zhang, L.; Xiao, Y.; Zhang, L.; Xing, Y. Effect of TongmaiYangxin Pills on inflammatory factors and oxidative stress of cardiomyocyte injury induced by hypoxia. *J. Tradit. Chin. Med.* **2011**, *52*, 326−328.

(5) Cui, Y.; Li, C.; Zeng, C.; Li, J.; Zhu, Z.; Chen, W.; Huang, A.; Qi, X. Tongmai Yangxin pills anti-oxidative stress alleviates cisplatin-induced cardiotoxicity: Network pharmacology analysis and experimental evidence. *Biomed. Pharmacother.* **2018**, *108*, 1081−1089.

(6) Pan, L.; Li, Z.; Wang, Y.; Zhang, B.; Liu, G.; Liu, J. Network pharmacology and metabolomics study on the intervention of traditional Chinese medicine Huanglian Decoction in rats with type 2 diabetes mellitus. *J. Ethnopharmacol.* **2020**, *258*, No. 112842.

(7) Chen, Y.-X.; Zhang, X.; Huang, J.; Zhou, S.; Liu, F.; Jiang, L.; Chen, M.; Wan, J.; Yang, D. UHPLC/Q-TOFMS-based plasma metabolomics of polycystic ovary syndrome patients with and without insulin resistance. *J. Pharm. Biomed. Anal.* **2016**, *121*, 141−150.

(8) Li, Y.; Deng, H.; Ju, L.; Zhang, X.; Zhang, Z.; Yang, Z.; Wang, L.; Hou, Z.; Zhang, Y. Screening and validation for plasma biomarkers of nephrotoxicity based on metabolomics in male rats. *Toxicol. Res.* **2016**, *5*, 259−267.

(9) Falvo, J. V.; Jasenosky, L. D.; Kruidenier, L.; Goldfeld, A. E.Epigenetic Control of Cytokine Gene Expression: Regulation of the TNF/LT Locus and T Helper Cell Differentiation. In *Advances in Immunology*; Elsevier, 2013; Vol. *118*, pp 37−128.

(10) Wu, Q.; Huang, Q. X.; Zeng, H. L.; Ma, S.; Lin, H. D.; Xia, M. F.; Tang, H. R.; Gao, X. Prediction of Metabolic Disorders Using NMR-Based Metabolomics: The Shanghai Changfeng Study. *Phenomics* **2021**, *1*, 186−198.

(11) Jiang, M.; Lu, C.; Zhang, C.; Yang, J.; Tan, Y.; Lu, A.; Chan, K. Syndrome differentiation in modern research of traditional Chinese medicine. *J. Ethnopharmacol.* **2012**, *140*, 634−642.

(12) Li, Y.; Li, Y.; Lu, W.; Li, H.; Wang, Y.; Luo, H.; Wu, Y.; Dong, W.; Bai, G.; Zhang, Y. Integrated Network Pharmacology and Metabolomics Analysis of the Therapeutic Effects of Zi Dian Fang on Immune Thrombocytopenic Purpura. *Front. Pharmacol.* **2018**, *9*, No. 597.

(13) Huang, W.; Liu, C.; Xie, L.; Wang, Y.; Xu, Y.; Li, Y. Integrated network pharmacology and targeted metabolomics to reveal the mechanism of nephrotoxicity of triptolide. *Toxicol. Res.* **2019**, *8*, 850−861.

(14) Lopaschuk, G. D.; Ussher, J. R.; Folmes, C. D.; Jaswal, J. S.; Stanley, W. C. Myocardial fatty acid metabolism in health and disease. *Physiol. Rev.* **2010**, *90*, 207−258.

(15) Wen, J.-J.; Garg, N. Oxidative modification of mitochondrial respiratory complexes in response to the stress of Trypanosoma cruzi infection. *Free Radical Biol. Med.* **2004**, *37*, 2072−2081.

(16) Lei, P.; Mwangi, C. N.; Cao, Y. L.; Chen, J. R.; Huang, Y. T.; Wang, Y. F.; Zhu, Y.; Fan, G. W.; Jiang, M. M. Investigating the mechanism of action of Danhong injection and its components against myocardial ischemia-reperfusion injury. *Acupunct. Herb. Med.* **2023**, No. 10-1097.

(17) Taegtmeyer, H.; Harinstein, M. E.; Gheorghiade, M. More than bricks and mortar: comments on protein and amino acid metabolism in the heart. *Am. J. Cardiol.* **2008**, *101*, S3−S7.

(18) Liu, G.; Chen, S.; Zhong, J.; Teng, K.; Yin, Y. Crosstalk between Tryptophan Metabolism and Cardiovascular Disease, Mechanisms, and Therapeutic Implications. *Oxid. Med. Cell. Longevity* **2017**, *2017*, 1−5.

(19) Mangge, H.; Summers, K. L.; Meinitzer, A.; Zelzer, S.; Almer, G.; Prassl, R.; Schnedl, W. J.; Reininghaus, E.; Paulmichl, K.; Weghuber, D.; Fuchs, D. Obesity-related dysregulation of the tryptophan-kynurenine metabolism: role of age and parameters of the metabolic syndrome. *Obesity* **2014**, *22*, 195−201.

(20) Huang, H.; Vandekeere, S.; Kalucka, J.; Bierhansl, L.; Zecchin, A.; Bruning, U.; Visnagri, A.; Yuldasheva, N.; Goveia, J.; Cruys, B.; Brepoels, K.; Wyns, S.; Rayport, S.; Ghesquiere, B.; Vinckier, S.; Schoonjans, L.; Cubbon, R.; Dewerchin, M.; Eelen, G.; Carmeliet, P. Role of glutamine and interlinked asparagine metabolism in vessel formation. *EMBO J.* **2017**, *36*, 2334−2352.

(21) Crespo, I.; San-Miguel, B.; Prause, C.; Marroni, N.; Cuevas, M. J.; Gonzalez-Gallego, J.; Tunon, M. J. Glutamine treatment attenuates endoplasmic reticulum stress and apoptosis in TNBS-induced colitis. *PLoS One* **2012**, *7*, No. e50407.

(22) Kim, Y. S.; Jung, M. H.; Choi, M. Y.; Kim, Y. H.; Sheverdin, V.; Kim, J. H.; Ha, H. J.; Park, D. J.; Kang, S. S.; Cho, G. J.; Choi, W. S.; Chang, S. H. Glutamine attenuates tubular cell apoptosis in acute kidney injury via inhibition of the c-Jun N-terminal kinase phosphorylation of 14-3-3. *Crit. Care Med.* **2009**, *37*, 2033−2044.

(23) Cao, S.; Xu, W.; Zhang, N.; Wang, Y.; Luo, Y.; He, X.; Huang, K. A mitochondria-dependent pathway mediates the apoptosis of GSE-induced yeast. *PLoS One* **2012**, *7*, No. e32943.
(24) Cazanave, S. C.; Mott, J. L.; Elmi, N. A.; Bronk, S. F.; Werneburg, N. W.; Akazawa, Y.; Kahraman, A.; Garrison, S. P.; Zambetti, G. P.; Charlton, M. R.; Gores, G. J. JNK1-dependent PUMA expression contributes to hepatocyte lipoapoptosis. *J. Biol. Chem.* **2009**, *284*, 26591−26602.
(25) Malhi, H.; Bronk, S. F.; Werneburg, N. W.; Gores, G. J. Free fatty acids induce JNK-dependent hepatocyte lipoapoptosis. *J. Biol. Chem.* **2006**, *281*, 12093−12101.
(26) Takahashi, M.; Okazaki, H.; Ogata, Y.; Takeuchi, K.; Ikeda, U.; Shimada, K. Lysophosphatidylcholine induces apoptosis in human endothelial cells through a p38-mitogen-activated protein kinase-dependent mechanism. *Atherosclerosis* **2002**, *161*, 387−394.
(27) Wang, Y.; Wang, Y.; Li, G. TRPC1/TRPC3 channels mediate lysophosphatidylcholine-induced apoptosis in cultured human coronary artery smooth muscles cells. *Oncotarget* **2016**, *7*, 50937−50951.
(28) Zuo, X. Y.; Yao, R. F.; Zhao, L. Y.; Zhang, Y. J.; Lu, B. N.; Pang, Z. R. Campanumoea javanica Bl. activates the PI3K/AKT/mTOR signaling pathway and reduces sarcopenia in a T2DM rat model. *Acupunct. Herb. Med.* **2022**, *2*, 99−108.
(29) Young, M. M.; Kester, M.; Wang, H. G. Sphingolipids: regulators of crosstalk between apoptosis and autophagy. *J. Lipid Res.* **2013**, *54*, 5−19.
(30) Liao, J.; Guan, Y.; Chen, W.; Shi, C.; Yao, D.; Wang, F.; Lam, S. M.; Shui, G.; Cao, X. ACBD3 is required for FAPP2 transferring glucosylceramide through maintaining the Golgi integrity. *J. Mol. Cell Biol.* **2019**, *11*, 107−117.
(31) Hannun, Y. A.; Obeid, L. M. Sphingolipids and their metabolism in physiology and disease. *Nat. Rev. Mol. Cell Biol.* **2018**, *19*, 175−191.
(32) Zhou, B.; Zhan, H. Q.; Qin, Y. L.; Yuan, G.; Min, H. L. Assessment of pulmonary infectious disease treatment with Mongolian medicine formulae based on data mining, network pharmacology and molecular docking. *Chin. Herb. Med.* **2022**, *14*, 432−448.
(33) Takino, J. I.; Sato, T.; Nagamine, K.; Hori, T. The inhibition of Bax activation-induced apoptosis by RasGRP2 via R-Ras-PI3K-Akt signaling pathway in the endothelial cells. *Sci. Rep.* **2019**, *9*, No. 16717.
(34) Xin, L.; Xiao, W. J.; Hai, X. C.; Qing, C. Z.; Huai, W. D.; Chao, H. C. Neuroprotective effects of kukoamine A on 6-OHDA-induced Parkinson's model through apoptosis and iron accumulation inhibition. *Chin. Herb. Med.* **2021**, *13*, 105−115.
(35) Zhou, Z.; Lu, X.; Wang, J.; Xiao, J.; Liu, J.; Xing, F. MicroRNA let-7c is essential for the anisomycin-elicited apoptosis in Jurkat T cells by linking JNK1/2 to AP-1/STAT1/STAT3 signaling. *Sci. Rep.* **2016**, *6*, No. 24434.
(36) Huang, Y.; Liu, N.; Liu, J.; Liu, Y.; Zhang, C.; Long, S.; Luo, G.; Zhang, L.; Zhang, Y. Mutant p53 drives cancer chemotherapy resistance due to loss of function on activating transcription of PUMA. *Cell Cycle* **2019**, *18*, 3442−3455.
(37) Hao, G.; Zhai, J.; Jiang, H.; Zhang, Y.; Wu, M.; Qiu, Y.; Fan, C.; Yu, L.; Bai, S.; Sun, L.; Yang, Z. Acetylshikonin induces apoptosis of human leukemia cell line K562 by inducing S phase cell cycle arrest, modulating ROS accumulation, depleting Bcr-Abl and blocking NF-κB signaling. *Biomed. Pharmacother.* **2020**, *122*, No. 109677.
(38) Pistritto, G.; Trisciuoglio, D.; Ceci, C.; Garufi, A.; D'Orazi, G. Apoptosis as anticancer mechanism: function and dysfunction of its modulators and targeted therapeutic strategies. *Aging* **2016**, *8*, 603−619.
(39) Zhang, Y.; Chen, S.; Fan, F.; Xu, N.; Meng, X. L.; Zhang, Y.; Lin, J. M. Neurotoxicity mechanism of aconitine in HT22 cells studied by microfluidic chip-mass spectrometry. *J. Pharm. Anal.* **2023**, *13*, 88−98.
(40) Tao, S.; Huang, Y.; Chen, Z.; Chen, Y.; Wang, Y.; Wang, Y. Rapid identification of anti-inflammatory compounds from Tong-maiYangxin Pills by liquid chromatography with high-resolution mass spectrometry and chemometric analysis. *J. Sep. Sci.* **2015**, *38*, 1881−1893.

https://doi.org/10.1021/acsomega.3c01441
ACS Omega 2023, 8, 18128−18139